BIOORGANIC CHEMISTRY 23, 263–300 (1995)

CONFERENCE PROCEEDINGS

Fourteenth Enzyme Mechanisms Conference

RONALD KLUGER* AND GORDON A. HAMILTON†

*Department of Chemistry, University of Toronto, Toronto, Ontario M5S 1A1, Canada; and
†Department of Chemistry, Pennsylvania State University, University Park, Pennsylvania 16802

Received May 12, 1995

The Fourteenth Biennial Conference on Enzyme Mechanisms, organized by C. Dale Poulter (chair), John W. Kozarich, David E. Cane, Rowena G. Matthews, and Christian P. Whitman, was held on January 5–8, 1995 at Scottsdale, Arizona. A total of 21 formal talks covering a broad array of topics in the general areas of enzyme mechanisms and bioorganic chemistry were given. In addition, two poster sessions were held with a total of 100 posters being presented. In the following, a brief synopsis of each of the major talks, as well as a few select references to recent work in the area of the talk, is given. Also, the titles and authors of the posters are listed. It is hoped that this brief summary of the meeting not only will indicate the types of studies currently of interest to mechanism-oriented bioorganic chemists, but also will serve as a starting point for those who wish to delve more deeply into the topics that were discussed.

1. MAGNETIC FIELD EFFECTS IN B_{12} ENZYMATIC REACTIONS

In the first presentation, Charles B. Grissom from the University of Utah outlined a theory of magnetic field effects in chemical and enzymatic reactions based on radical-pair intermediates. He showed that the steady-state and stopped-flow kinetic parameters of B_{12}-dependent ethanolamine ammonia lyase from *Salmonella typhimurium* depend upon the applied magnetic field (0–2000 gauss). This is the first convincing report of a magnetic field effect on the kinetics of an enzymatic reaction (*1–3*).

A magnetic field can affect the rate of a chemical reaction by changing the rate of intersystem crossing between the singlet and triplet state in a radical pair (Fig. 1). Only the singlet radical pair $\{R\cdot\ \cdot R'\}$ can recombine to form starting material. In order for the rate of an enzymatic reaction with radical intermediates to be affected by a magnetic field, a pair of radicals must be formed reversibly during the catalytic cycle. The underlying theory of magnetic field effects in enzymatic reactions has been described elsewhere by Grissom (*4*).

In the case of B_{12}-dependent ethanolamine ammonia lyase, the kinetic parameter V_{max}/K_m is decreased by 25% at 1000 gauss (G) with unlabeled ethanolamine as substrate and 60% at 1200 G with perdeuterated ethanolamine as substrate (*1*). Stopped-flow kinetic studies reveal the magnetic field-dependent step to be recombination of the radical pair (5′-deoxyadenosyl radical and cob(II)alamin) at the beginning of the catalytic cycle (*2*). This observation is supported by magnetic field-

0045-2068/95 $12.00

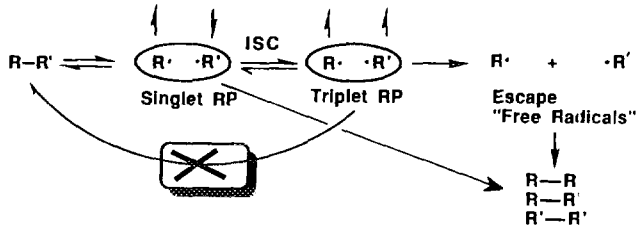

FIG. 1. Magnetic field effects in radical reactions.

dependent recombination of this same radical pair produced by photolysis of adenosylcob(III)alamin (*3*).

The magnetic field dependence of the steady-state and stopped-flow kinetic parameters offers a new technique for studying the mechanism of enzymes with radical pair intermediates. The *g*-value, hyperfine coupling constant, and kinetic rate information reflect the physical parameters of the kinetically competent radical pair during catalysis.

2. FORMATION OF C-TERMINAL AMIDE FUNCTIONALITY IN MAMMALIAN AND INSECT PEPTIDES

A mechanistically interesting biosynthetic pathway was the focus of the talk by John Vederas of the University of Alberta. Many biologically important neuropeptides have a C-terminal amide functionality, which is formed from a glycine-extended precursor in a two-step process catalyzed by amidating enzymes. These enzymes may occur either as a single bifunctional protein, peptidyl-glycine α-amidating monooxygenase (PAM), or as two separately derived proteins, peptidyl-glycine α-hydroxylating monooxygenase (PHM) and peptidyl-α-hydroxyglycine α-amidating lyase (PAL), which catalyze the reactions shown in Fig. 2 (*5*). PHM requires copper (two in the active site), dioxygen, and ascorbate, as does dopamine β-hydroxylase. Vederas and his group have accomplished the first purification and characterization of PHM from an invertebrate, the honeybee *Apis mellifera* (*6*). This PHM, which was isolated from honey bee heads, is much more lipophilic and larger (MW ca. 63,500) than corresponding mammalian PHM enzymes. Selective inhibitors which do not affect corresponding amidating enzymes in animals may be effective pest

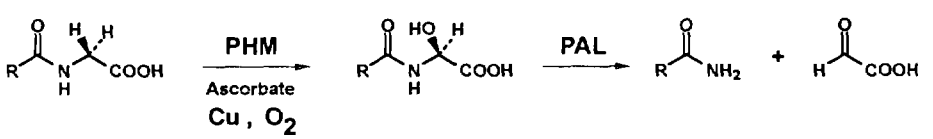

FIG. 2. Reactions catalyzed by peptide α-amidating enzymes.

control agents since insect neuropeptides control critical functions (*7*). Labeling studies elucidated the stereochemistry of bee PHM, defining limits on the mechanism. Three types of mechanism based inhibitors were synthesized and tested against both mammalian and insect PHM (*6, 8*). In each case, there is possible delocalization of an initially formed carbon-based radical. Vederas proposes that inactivation could occur by electron transfer processes from this radical to generate potent electrophiles that attack active site residues.

3. FINASTERIDE: A POTENT MECHANISM-BASED INHIBITOR OF 5α-REDUCTASE

Georgianna Harris of Merck Research Laboratories presented mechanistic insights gathered from a project undertaken together with Herb Bull on one of Merck's most important new drugs, finasteride (formulated as Proscar) or (*N*-(1,1-dimethylethyl)-3-oxo-4-aza-5α-andros-1-ene-17β-carboxamide). Finasteride is an inhibitor of 5α-reductase, the enzyme responsible for the conversion of testosterone to dihydrotestosterone. This inhibitor is used clinically to treat benign prostatic hyperplasia (enlargement). Previous studies have shown that finasteride is a slow-binding inhibitor of human type 2 (prostate) 5α-reductase (*9*). It binds to the enzyme–NADPH complex with a rate constant of $\sim 3 \times 10^5$ M^{-1} s^{-1}, which is at least an order of magnitude slower than diffusion controlled and even slower than the corresponding rate constant for reduction of testosterone ($k_{cat}/K_m = \sim 1 \times 10^6$ M^{-1} s^{-1}). The resulting enzyme–inhibitor complex is extremely stable. The half-life of the type-2 enzyme–inhibitor complex is ≥30 days at 37°C ($k = 3 \times 10^{-7}$ s^{-1}), based on the rate of release of radioactivity from enzyme–[^{3}H]finasteride complex, conducted using crude, membrane-bound preparations of the enzyme. For a reversible system, the rate constants for formation and dissociation of the complex indicate $K_i = k_{off}/k_{on} = -1$ pM.

Remarkably, the released radioactivity does not elute with finasteride but with its reduction product, dihydrofinasteride; identification of the product as dihydrofinasteride was established by mass spectrometry. The formation of dihydrofinasteride cannot account for the potent inhibition by finasteride since dihydrofinasteride is a reversible inhibitor of the type 2 enzyme with $K_i = \sim 10$ nM. Furthermore, the inhibitor appears to be concovalently bound to the enzyme, since denaturation of the enzyme–[^{3}H]inhibitor complex in guanidine hydrochloride quantitatively releases the radiolabel. Yet, the material released by denaturation is not dihydrofinasteride; the properties are consistent with a covalent complex of dihydrofinasteride and $NADP^+$. Precedent for enzyme-catalyzed production of a covalent complex of an oxidized pyridine nucleotide and product comes from the work of Kaplan and co-workers (*10*). They observed that lactate dehydrogenase catalyzes the addition of pyruvate to NAD^+.

Finasteride has also been described as a time-dependent inhibitor of the human type 1 (scalp) isozyme (*11*). With this isozyme, finasteride is a much slower time-dependent inhibitor ($k_{on} = \sim 1 \times 10^3$ M^{-1} s^{-1}). Dr. Harris showed that the type 1 isozyme also catalyzes reduction of finasteride to dihydrofinasteride and adduct

formation with $NADP^+$. As found with the type 2 enzyme, there is no evidence for recovery of catalytic activity from this enzyme–inhibitor complex. The two orders of magnitude difference in the second order rate constants results in the selectivity of finasteride for the type 2 reductase observed clinically. In essence, finasteride is an elegant mechanism-based inhibitor of both human isozymes of 5α-reductase!

4. INHIBITION OF CARBOHYDRATE-MEDIATED CELL ADHESION

Chi-Huey Wong of the Scripps Research Institute reported on his work elucidating the role played by complex carbohydrates on cell surfaces in biochemical recognition (*12–15*). Partially because of the difficulty associated with the synthesis and analysis of this class of molecules little is known about them even though they are critically needed for the study of enzymes (e.g., glycosidases and glcosyltranferases) involved in their processing and synthesis. Dr. Wong's efforts in this regard are directed toward the development of molecules to control the cell adhesion process mediated by the interaction of sialyl Lewis X and E-selectin. The minimum topostructure of sialyl Lewis X recognized by E-selectin has been determined and the enzymes associated with the biosynthesis have been studied with regard to their substrate specificity and inhibition. Many azasugar inhibitors of α-1,3-fucosyltransferase have been designed and synthesized to probe the active site of the enzyme responsible for the last step in the biosynthesis of the blood antigen sialyl Lewis X. Furthermore, Dr. Wong and his group have prepared and evaluated transition state analogs containing an azasugar as the glycosyl donor and a manganese pyrophosphate mimic as inhibitors of α-1,3-fucosyltransferase.

5. STRUCTURE, FUNCTION, INHIBITION OF PROSTAGLANDIN ENDOPEROXIDE SYNTHASES

Lawrence J. Marnet of Vanderbilt University summarized some recent research that he and his group have done in this area (*16, 17*). Prostaglandin endoperoxide synthase (PGHS) catalyzes (Fig. 3) the oxygenation of arachidonic acid to the hydroperoxy endoperoxide, PGG_2, (cyclooxygenase activity) and the reduction of PGG_2 to the hydroxy endoperoxide, PGH_2 (peroxidase activity). Peroxidase higher oxidation states play a role in activating cyclooxygenase activity presumably by formation of protein radicals that serve as initiators of arachidonic acid oxidation. Attention has focused on tyrosyl radicals that have been detected during cyclooxygenase and peroxidase turnover by EPR spectroscopy. However, evidence for the involvement of spectroscopically detectable tyrosyl radicals as catalytically competent intermediates is controversial.

Cysteinyl radicals are highly reactive toward arachidonic acid in solution so Dr. Marnett's group investigated the possibility that cysteinyl radicals are catalytic intermediates in cyclooxygenase turnover. Peptide mapping revealed that there are three free cysteines in PGHS (from a total of 13). These residues are C313, C512,

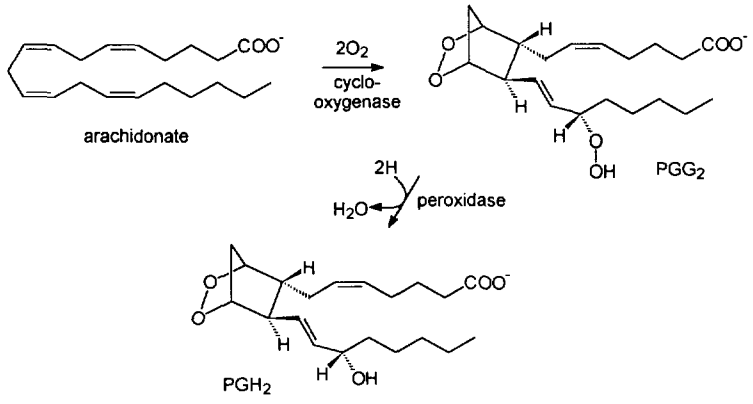

FIG. 3. Reactions catalyzed by prostaglandin endoperoxide synthase.

and C540. *N*-ethylmaleimide (NEM) inactivates cyclooxygenase and peroxidase activities of holoPGHS in a time-dependent manner, but does not affect apoPGHS. Peptide mapping demonstrated that NEM reacts primarily with C313 in holoPGHS and with C540 in apoPGHS. Each of the three cysteines was changed to serine by site-directed mutagenesis and the mutant proteins were expressed in COS-1 cells. The C512S mutant converts arachidonic acid to products to the same extent as wild-type PGHS. In contrast, the C313S and C540S mutants convert arachidonic acid to products to the extent of 10% of wild-type PGHS. These results indicate that C313, C512, and C540 are not essential for cyclooxygenase activity but that alteration of C540 or C313 dramatically decreases enzyme activity. Both residues are well-removed from the cyclooxygenase and preoxidase active sites so the findings reveal that subtle changes, such as substitution of a single oxygen for a sulfur atom as far as 30 Å from the heme prosthetic group, can significantly alter enzyme activity.

Although several different maleimides inactivate the cyclooxygenase and peroxidase activities of PGHS, high concentrations of maleimide are required and the rate of inactivation is slow. An attempt was made to improve the potency of maleimides as inhibitors by tethering groups to the maleimide nitrogen that are designed to improve the affinity of the inhibitors for the cyclooxygenase active site. *N*-(carboxyalkyl)maleimides were found to inactivate cyclooxygenase and peroxidase activities of PGHS in a biphasic manner with extremely rapid inactivation followed by slow time-dependent inactivation. The carboxylic acid moiety was required for rapid inactivation. Optimal inhibition was observed with *N*-(carboxyheptyl)maleimide which inhibits the cyclooxygenase activity of ovine PGHS-1 at concentrations stoichiometric with protein. *N*-(carboxyheptyl)succinimide inhibits neither enzyme activity, suggesting that covalent modification is critical for rapid and time-dependent inactivation. Shortening or increasing the alkyl chain by one methylene unit drastically reduced inhibitory potency. *N*-(carboxyalky)maleimides also instantaneously inactivated the inducible form of PGHS (PGHS-2) from mouse and human sources but with higher IC_{50}s. *N*-(carboxyheptyl)maleimide is the most

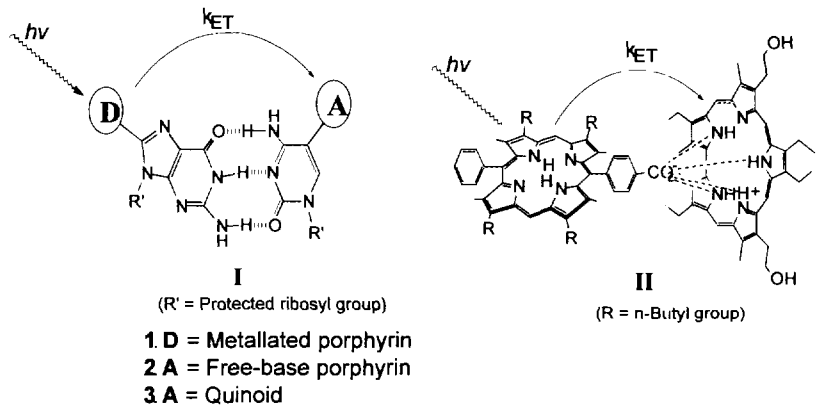

FIG. 4. Photosynthetic modeling systems.

potent covalent inactivator of PGHS yet described with an inhibitory potency three to five orders of magnitude greater than that of aspirin. Interestingly, the three cysteine-to-serine mutant PGHSs described above are inhibited by *N*-(carboxyheptyl)maleimide at concentrations comparable to that of wild-type enzyme, implying that cysteines are not the target residues for modification leading to loss of enzyme activity.

6. NONCOVALENT ELECTRON TRANSFER MODEL SYSTEMS

Further elaboration of a new approach to photosynthetic modeling involving the construction and manipulation of purine- and pyrimidine-derived systems (*18–22*) was reported by Jonathan L. Sessler of the University of Texas at Austin. In particular, the syntheses and photophysical properties of several rigid guanine– and cytosine–porphyrin and quinone systems, such as **1, 2,** and **3** (see Fig. 4) were described. Furthermore, evidence that supports the contention that these and other related systems undergo self-association in CH_2Cl_2 to produce hydrogen bonded conjugates, such as **I**, that are photoactive with regard porphyrin-to-porphyrin energy transfer or porphyrin-to-quinone electron transfer was presented (*18–22*).

Also presented for the first time was a new approach to the construction of noncovalent electron transfer model systems that is predicated on the use of carboxylate anion-to-protonated sapphyrin salt bridges. This approach, embodied in the photoactive supramolecular assembly **II,** is allowing an evaluation of this type of interaction in terms of its ability to mediate long-distance energy and/or electron transfer processes under well-defined laboratory conditions.

7. NONTRADITIONAL ROLES OF WATER IN ENZYME RECOGNITION AND CATALYSIS

Stephen Sligar of the University of Illinois at Urbana presented an expanded view on roles for solvent water in enzyme recognition and catalytic function (*23–27*). Over the past decade, the use of hydrostatic and osmotic pressure to study biological

macromolecular conformation and interactions has become widespread. Pressure represents an ideal variable either on its own, or as a complement to the more traditional variables such as temperature and pH, since variation of pressure enables the calculation of reaction and activation volumes for critical steps in recognition and catalysis. By manipulating hydrostatic pressure, one may perturb the volume of a system without simultaneously creating changes in the internal energy (as occurs with temperature) or the solvent composition (as with pH or chaotropic agents). In addition, effects of osmotic pressure are uniquely useful in identifying reactions involving solvent water binding or release. Used in conjunction, osmotic and hydrostatic pressure can provide unique information regarding volume changes and hydration effects involved in phenomenon such as protein or nucleic acid denaturation, protein–protein and protein–small molecule interactions, nucleic acid–protein interactions, and other classes of macromolecular structural transitions and recognition events.

Pressure manipulations involve intuitive thermodynamic concepts: the response of a system to hydrostatic pressure is to minimize volume; the response of a system to osmotic pressure is to minimize bound water. Since the compressibility of protein–water interfaces is much greater than that of bulk water, hydrostatic pressure promotes the dissociation of oligomers or complexes (by favoring solvation of interfacial domains) and disruption of the folded, native conformation of single-chain, globular, monomeric proteins. Conversely, induction of osmotic pressure arises from a difference in chemical potential between water molecules in bulk solvent and waters sequestered from bulk solvent in a protein surface cleft, cavity, or interface, which can result in the release of waters to bulk solvent to equilibrate chemical potential. Thus pressure techniques provide a probe for assessing the role of bound waters in many biophysical and biochemical processes.

One area where water structure, particularly hydrogen bonded networks of active site waters, is critical to catalysis is in the cytochrome P-450-dependent mixed function oxidases which play central and crucial roles in mammalian, plant, insect, viral, and microbial metabolism. All P-450 catalyzed monoxygenase reactions reduce atmospheric dioxygen producing water and a monoxygenated substrate. A central question related to the mechanisms of these important biological oxidations include the precise chemistry involved in activation of oxygen and substrate and the identity of metal–oxygen–carbon intermediates in the catalytic event. Using a combination of solvent kinetic isotope effects, site-directed mutagenesis, and osmotic pressure techniques, Dr. Sligar documented a critical role for hydrogen-bonded solvent networks in the distal pocket of the cytochrome P450s in the activation and cleavage of heme bound dioxygen. Figure 5 shows participation of Asp251 and Thr252 in the P-450cam active site, forming a charge relay system which utilizes the formation of low-barrier hydrogen bonds to aid in the scission of the oxygen–oxygen bond. In the case of those cytochrome P450s which lack an amino acid-based hydroxyl, it appears that a network of hydrogen-bonded waters could provide an equivalent low barrier ("strong") hydrogen bond for dioxygen bond scission.

A second example of the nontraditional roles of water is in the mediation of protein–DNA interactions. Protein–nucleic acid interactions are of key importance in many biological and biochemical processes. Hydrostatic and osmotic pressure methods have begun to make major contributions in dissecting the origins of speci-

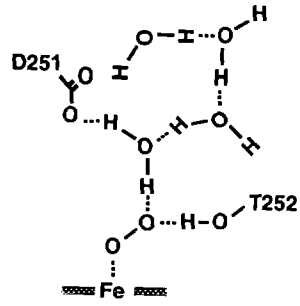

FIG. 5. Hydrogen bonded structure at the active site of P450cam.

ficity of these interactions, particularly the role played by water in DNA site discrimination. Restriction endonucleases represent a paradigm for site-specific DNA recognition by proteins. Under standard conditions, Type II restriction enzymes cleave their canonical recognition sequences about 10^6 times faster than any other sequence. Changes in the buffer conditions, however, can lead to cleavage at alternate sites, termed "star" sites. In the *Eco*RI endonuclease system, the extent of cleavage at these star sites was measured in the presence of neutral solutes and cosolvents.

Dr. Sligar finds a correlation between osmotic pressure (in the range from 0 to 100 atm) and the change in *Eco*RI specificity manifest as "star" site cleavage. A wide variety of compounds were tested to confirm that, other than osmotic pressure, colligative solvent properties, such as viscosity, dielectric constant, or water molarity are not uniformly correlated with the change in enzyme specificity. Application of hydrostatic pressures up to 400 atm reversed, and ultimately eliminated, the effects of osmotic pressure, restoring the natural selectivity of the enzyme (Fig. 6).

These observations lead to a model where water molecules associated with the protein–DNA complex assist in accurate recognition of the canonical GAATTC site. Osmotic pressure releases these waters, leading to a change in the specificity of the enzyme. Hydrostatic pressure is believed to resolvate the system, thus restoring the natural selectivity of the enzyme. By determining the values of K_m and k_{cat} as a function of osmotic pressure, volume changes were calculated for the association and catalytic steps of the reaction at canonical (GAATTC) and star (TAATTC) sites. Assuming a constant density for all water molecules, these volume changes correspond to release of approximately 160 waters upon binding at the canonical site and 200 waters upon binding at the star site, implying that about 40 waters are present in the complex at the canonical site which are not present at the "star" site. Furthermore, elevated osmotic pressure results in a decrease in k_{cat} at the canonical site corresponding to the binding of about 25 waters during catalysis, whereas k_{cat} at the star site increases with osmotic pressure, indicative of release of an additional 45 hydration waters. Thus, water appears to participate in recognition during the binding and catalytic phases of the reaction. Moreover, the release of water results in a fundamental change in the selectivity of the enzyme, as the canonical site becomes less favored as a substrate with increasing osmotic pressure.

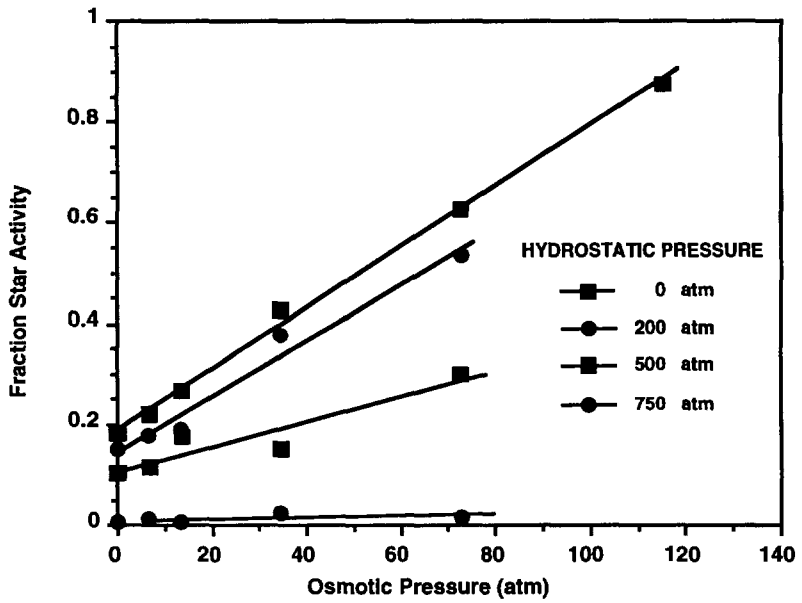

FIG. 6. Reversal of *Eco*RI* activity by hydrostatic pressure.

This motif of differential solvation is also utilized by other restriction enzymes, such as *Bam*HI and *Pvu*II. Despite belonging to different structural subclasses of Type II restriction enzymes, these two enzymes respond in the same way as *Eco*RI to osmotic and hydrostatic pressure. Osmotic pressure induces a uniform change in specificity, while hydrostatic pressure counteracts these effects. Intriguingly, although *Eco*RV belongs to the same structural family as *Pvu*II, its specificity is not affected by osmotic pressure; no *Eco*RV* activity is induced by addition of osmolytes to the reaction buffer. Thus, the participation of bound water in recognition is a mechanism which is not limited to, nor defined by the emerging structural classes of restriction enzymes.

The main conclusion to be derived from Dr. Sligar's presenation is that solvent waters play important roles in enzyme mechanisms aside from that of solubilization of the macromolecule. Furthermore, hydrostatic and osmotic pressure are key techniques in understanding the structure–function relationships for these uses of hydrogen bonded solvent networks in both catalysis and recognition.

8. ENZYMES AND ABZYMES

The theme of the talk given by Stephen J. Benkovic of the Pennsylvania State University was catalysis. Although we primarily think of catalysis in terms of transition state stabilization, Dr. Benkovic reminded the audience that that concept is

at best an oversimplification. For example, given the fact that transition states are known to have lifetimes on the order of femtoseconds, how do we imagine that the interaction between the enzyme and the substrate occurs? This issue was examined with evidence from enzymes and catalytic antibodies (*28–31*).

Because of the wealth of structural and kinetic information available, dihydrofolate reductase served as the enzymic paradigm. Site-specific mutagenesis of pairs of residues whose distance apart is far greater than van der Waals radii showed surprisingly nonadditive free energies in key kinetic and thermodynamic parameters that measured single events, such as cofactor binding or the chemical rate of hydride transfer. In addition, despite extensive changes, which reduced the interactions between the protein and the bound substrate, more activity of the enzyme was retained than anticipated. Moreover, 2d NMR measurements on ^{15}N isotopically substituted protein (all the amino acid assignments had been made previously) provided effective correlation times, order parameters, and exchange relaxation terms for greater than 95% of the backbone amide nitrogens. Of special interest was the finding of picosecond motions and lower order parameters associated with loop regions of the molecule previously implicated as important in maintaining the rate of the chemical transfer step. Especially striking was the observation of microsecond motions in secondary structural elements which flank the active site. Although the data do not reveal whether these latter motions are correlated, one is tempted to believe that they are. One interpretation of the data is that the faster motions are linked to "transition state stabilization" and the slower ones to ground-state effects that "create" the optimal free energy pathway along the reaction coordinate.

In short, generalizing from this case, the active site elements of an enzyme are highly interactive, exhibit a molecular redundancy through multiple interactions with its substrates, and show molecular motions that may be directly coupled to catalysis.

Catalytic antibodies now have been found for some 60+ reactions. Their rate accelerations range from a hundred- to a million-fold above background. They are generally highly stereospecific and are generated from a collection of 25–50 monoclonals. Recently Dr. Benkovic and his group showed that, using an antibody combinatorial library in phage, they could screen this collection of some million potential catalysts directly for their catalytic activity by their ability to complement an auxotrophic bacterium. The lesion is a decarboxylating enzyme in the pyrimidine biosynthetic pathway. This success provided the researchers with a statistically meaningful measurement of the odds of finding a catalyst (about 1 of 200) and also a superior catalyst with a rate acceleration of one hundred million.

Given this advance, what parameter, if any single one, determines the activity above background of the abzyme? Dr. Benkovic found that all 60+ reactions showed a logarithmic correlation between the ratio of substrate to hapten binding (a transition state mimic) and the measured rate acceleration relative to background. This suggests that catalytic antibodies may provide a measure of "transition state stabilization" (the presumption in the development of the correlation). They are created from a small sampling of the reaction coordinate space conveyed in the design of the transition state mimic used to induce them. Unlike enzymes they

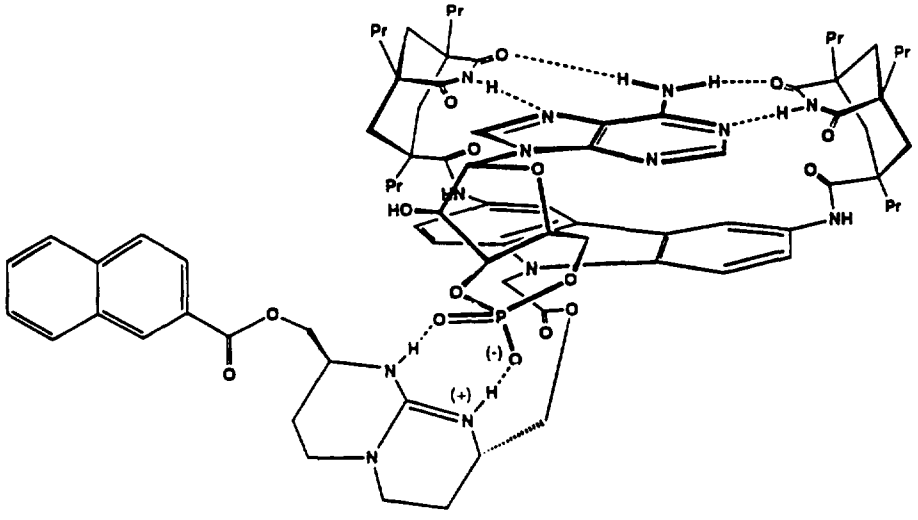

FIG. 7. Complex of a synthetic receptor with cyclic AMP.

cannot readily influence the course along the reaction coordinate. It is tempting to speculate that the superiority of enzymic catalysis is not only as others have argued in ground-state effects, but perhaps in molecular dynamics that are coupled into the reaction as it proceeds at the active site.

9. RECOGNITION AND REPLICATION IN MODEL SYSTEMS

Over the past few years Julius Rebek of the Massachusetts Institute of Technology has developed a number of synthetic receptors for small biorevelant targets. These generally feature what Dr. Rebek identifies as convergent functional groups with multiple recognition sites on a concave surface. For example, the structure shown in Fig. 7 features aromatic stacking, hydrogen bonding, and salt bridging elements in the recognition of cyclic AMP. These systems have been succeeded by complexes in which intramolecular reactions can take place and lead to catalysis. One peculiar form of this catalysis, autocatalysis, has been observed in synthetic receptors. Dr. Rebek went on to describe several other developments in self-replicating systems (*32–35*).

10. ENZYMOLOGY OF BACTERIAL LYSINE BIOSYNTHESIS

In his presentation John S. Blanchard of the Albert Einstein College of Medicine summarized recent studies performed in his laboratory on some of the enzymes that participate in bacterial lysine biosynthesis. Bacteria synthesize L-lysine from

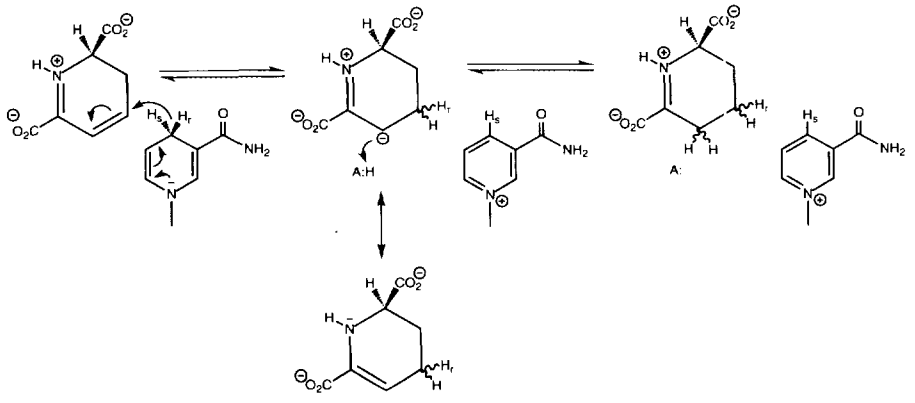

FIG. 8. Reaction catalyzed by dihydrodipicolinate reductase (DHPR).

L-aspartate and pyruvate via a nine-step biosynthetic scheme. The immediate precursor of lysine is *meso*-diaminopimelate, a component of gram negative peptidoglycan. The critical nature of these two amino acids, involved in protein and cell wall biosynthesis suggests that inhibitors of this pathway would be effective broad-spectrum antibacterials. One of the enzymes in this sequence, dihydrodipicolinate reductase (DHPR), catalyzes the NAD(P)H-dependent reduction (*36*) of the α,β-unsaturated cyclic imine, dihydrodipicolinate (2-keto-6-aminohept-3-ene-1,7-dioic acid) (Fig. 8). This enzyme has been the initial focus of Dr. Blanchard's enzymological and structural investigations. The *Escherichia coli* gene encoding DHPR, *dapB* (*37*), was overexpressed in BL21(DE3) cells, and the protein was purified to homogeneity. The enzyme exists as a tetramer of identical 29,000-Da monomers.

Initial velocity, product, and dead-end inhibition studies support an ordered kinetic mechanism with reduced pyridine nucleotide binding preceeding dihydrodipicolinate binding and with tetrahydrodipicolinate release preceeding oxidized nucletide release. NADH and NADPH exhibit nearly identical V/K values, and microcalorimetry demonstrated that NADH and NADPH bind to DHPR with K_d values of 0.26 and 1.8 μM, respectively. The enzyme catalyzes the transfer of the *pro*-R hydrogen from reduced pyridine nucleotide to the C_4 position of dihydrodipicolinate. Primary deuterium kinetic isotope effects on hydride transfer are nil, while the solvent kinetic isotope effect on the maximum velocity is 2.6. This suggests that the chemical mechanism is stepwise, with rapid hydride transfer to DHP yielding the eneamine, which tautomerizes in a slow proton transfer step to C_3 to form the reduced product.

The enzyme has been crystallized as the nucleotide binary complex from $(NH_4)_2SO_4$ by the hanging drop, vapor diffusion method; it crystallizes in the I222 space group. The structure was solved using two heavy atom derivatives and refined to 2.2 Å. The monmer is composed of an amino terminal, nucleotide binding domain and a carboxyl terminal domain which is involved in both tetramer assembly and substrate binding. The nucleotide substrate specificity is determined by two residues:

Arg39, which makes a single hydrogen bond to the 2′-phosphate of NADPH, and Asp38, which makes no interactions with the adenosyl ribose ring of NADPH, but two hydrogen bonds with the 2′ and 3′ hydroxyl groups of the adenosyl ribose ring of NADH. The active site cleft between the two domains is lined with histidine and lysine residues, generating a highly assymmetric surface charge distribution. Together the enzymological and structural information gained should provide information relevant to the evaluation of potent inhibitors of the enzyme.

11. MECHANISTIC STUDIES ON ENZYMES IN BACTERIAL PEPTIDOGLYCAN BIOSYNTHESIS

Christopher T. Walsh of the Harvard Medical School summarized ongoing investigations in his laboratory and in others with enzymes involved in bacterial cell wall biosynthesis (*38–43*). Again these are important potential targets for antibiotics. The chemical structure of the bacterial cell wall imparts rigidity to the cell, stabilizes it against osmotic lysis, and determines the bacterial cell shape. The major structural element of the cell wall is the polymeric peptidoglycan murein. The peptidoglycan polymer consists of alternating units of *N*-acetylglucosamine (GlcNAc) and *N*-acetylmuramic acid (MurNAc) with an attached pentapeptide. Precursors to the peptidoglycan are synthesized in the bacterial cytoplasm. The first committed step in the cell wall biosynthetic pathway is catalyzed by MurZ and involves the transfer of enolpyruvate from the phosphoenolpyruvate (PEP) to the 3′ hydroxyl of UDP–GlcNAc as depicted in Fig. 9, Scheme 1. Using biochemical and biophysical methods, including rapid-quench kinetics experiments, Walsh's group has isolated and characterized two reaction intermediates: (1) a covalent enzyme–phospholactyl adduct and (2) a phospholactyl UDP–GlcNAc tetrahedral intermediate (Fig. 9, Scheme 2).

Walsh and his group used the antibiotic fosfomycin and (*Z*)-3-fluorophosphoenolpyruvate (FPEP), analogs of PEP, as mechanistic probes of MurZ (Fig. 9, Scheme 3). The enzyme is irreversibly inactivated in a time and UDP–GlcNAc dependent manner by fosfomycin. The epoxide ring of fosfomycin is opened by the nucleophilic attack of an active site cysteine (Cys 115), resulting in a covalently modified enzyme that is inactive. The rate of formation and the breakdown of the tetrahedral intermediate is retarded when FPEP is used as a substrate instead of PEP. This suggests that the formation and breakdown of the tetrahedral intermediate proceeds through an oxocarbenium ion-like transition state. With FPEP the tetrahedral intermediate is formed without proceeding through the enzyme–phospholactyl adduct.

12. KINETICS AND MECHANISM IN RIBONUCLEASE MIMICS

In his presentation Ronald Breslow of Columbia University summarized some of his group's recent research on model reactions for ribonuclease catalysis (*44–47*). The hydrolysis of dinucleotides serves as a model for ribonuclease, but in the model 3′–2′ phosphate migration competes with hydrolysis. The addition of buffer

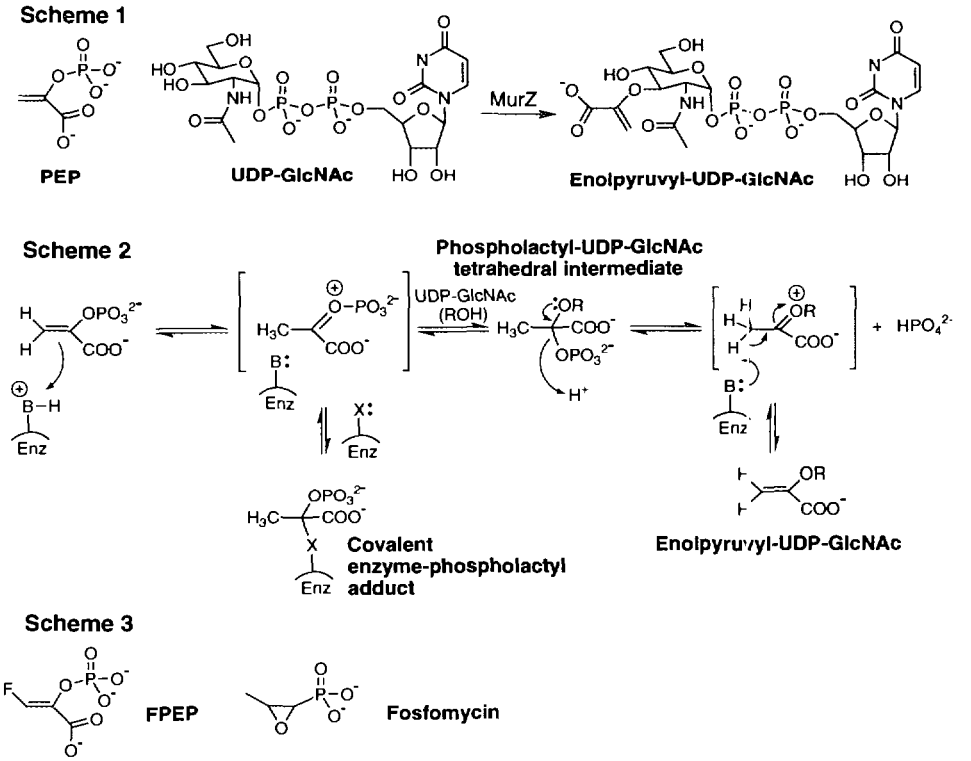

FIG. 9. Reactions, intermediates, and inhibitors in peptidoglycan biosynthesis.

promotes hydrolysis over migration. If one follows the appearance of the migrated phosphate, the buffer appears to decrease the rate of its formation. In fact, the yield decreases since the rate of consumption of the reactant is increased. The migration requires pseudorotation of the initial cyclic intermediate followed by hydrolysis while cleavage occurs without pseudorotation. Both formation of the intermediate and hydrolysis are buffer catalyzed while pseudorotation is not. Therefore, addition of buffer decreases the relative amount of migration product. Dr. Breslow calls the buffer a "negative catalyst" for migration but the term usually used for such phenomena is "inhibition."

In another aspect Dr. Breslow discussed his group's work on the cleavage of RNA catalyzed by imidazole buffer. Their data indicate that this reaction shows sequential bifunctional catalysis. When the two imidazole groups are attached to the same catalyst, as in enzymes or in cyclodextrin bis-imidazole derivatives, simultaneous bifunctional catalysis is seen. The geometric preference for such bifunctional catalysis is revealed by the use of three isomeric cyclodextrin bisimidazoles. Different isomers are preferred for phosphate ester hydrolysis and for ketone enolization, and the preferences reveal details of the catalytic mechanisms.

In very recent work Kirby and Marriott (*48*) have shown that the bell-shaped buffer plot that Dr. Breslow and his group have seen is an artifact of the medium at high buffer concentrations. Thus, apparently there is no term in both buffer components and the mechanism proposed by the Breslow group needs to be reconsidered.

13. DISSECTING CATALYSIS BY RIBONUCLEASE A

Ronald T. Raines of the University of Wisconsin presented the work of his group which reexamines the mechanism of ribonuclease A (RNase A; EC 3.1.27.5) using modern mutagenic and physical methods. Despite extensive study, the reaction energetics and the precise role of individual residues in catalysis by RNase A had been uncertain. The wealth of existing information of RNase A and the methods now available for manipulating both RNase A (*49*) and its substrates have made this system ideal for defining protein structure–function relationships in atomic detail.

Ribonuclease A catalyzes P–$O^{5'}$ bond hydrolysis in two steps: transphosphorylation of RNA to a 2′,3′-cyclic phosphodiester and hydrolysis of this cyclic phosphodiester to a 3′-phosphomonoester. Dr. Raines and his co-workers have shown that only 0.1% of an RNA substrate is both transphosphorylated and hydrolyzed without dissociating from the enzyme (*50*). RNase A catalyzes the transphosphorylation step by 10^{11}-fold, but the hydrolysis step by only 10^{8}-fold. These results indicate that RNase A has evolved primarily to catalyze RNA transphosphorylation rather than RNA hydrolysis.

Dr. Raines uses mutant and semisynthetic enzymes and synthetic substrates to delineate the contribution of each active-site residue (Fig. 10) to substrate recognition and turnover (*49, 51–53*). For example, his group has established (*51*) the value to catalysis of His12 (a general base) and His119 (a general acid), determined that the role of Lys41 is to donate one strong hydrogen bond to the transition state (*52*), and identified Gln11 as a residue that limits the nonproductive binding of substrate (*49*). Raines has found two new mutants of RNase A that catalyze the *processive* cleavage of RNA (*53*). This discovery has led to a new paradigm—a processive enzyme has subsites, each specific for a repeating motif within a polymeric substrate.

14. MECHANISTIC AND STRUCTURAL STUDIES ON DNA METHYLATION, DEMETHYLATION, AND REPAIR

In his presentation Gregory L. Verdine of Harvard University reviewed some of the background on the *Escherichia coli* Ada protein and then summarized some of his group's recent investigations designed to elucidate its detailed molecular mechanism of action. This protein is a central mediator of the adaptive response, a system whereby bacteria acquire resistance to the toxic and mutagenic effects of methylating agents (*54*). Ada repairs the mutagenic lesion O^{6}-methylguanine through direct, irreversible transfer of the methyl group to a cysteine residue (Cys_{321})

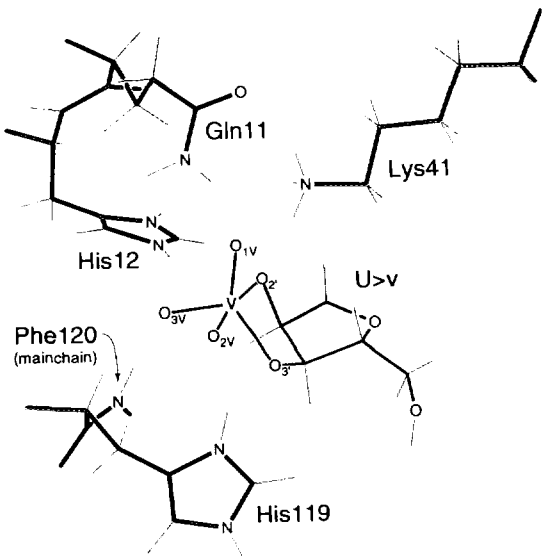

FIG. 10. Structure of the active site of RNase A bound to uridine 2′,3′-cyclic vanadate ($U > v$), a transition state analog. The sidechain of Phe120 and the base of $U > v$ are not shown.

located in the C-terminal domain of the protein (C-Ada19, Fig. 11). Ada also repairs the S_p diastereomer of methyl phosphotriesters in DNA; in this case, the methyl group is transferred to Cys_{69}, which lies within the N-terminal domain of the protein (N-Ada20). Upon methylation of Cys_{69}, a weak sequence-specific DNA-binding activity in Ada becomes greatly potentiated (*55*), thus endowing the protein with the ability to activate transcription of several genes, including that encoding Ada itself (*54, 56*). The protein products of the genes activated by Cys_{69}–me–Ada counter the adverse effects of methylating agents in a variety of ways, including direct removal of aberrant methyl groups (Ada) and glycolytic excision of methylated bases (AlkA) in duplex DNA.

Several years ago, Dr. Verdine and his group discovered that the Ada N-terminal domain contains a tightly bound zinc ion, which is required for folding of the protein *in vitro* and *in vivo* (*57*). Through a combined approach involving site-directed mutagenesis of prospective ligand residues and $[^1H]^{113}Cd$ correlation NMR experiments, they determined that the metal is coordinated to cysteine residues located at positions 38, 42, and 72. Unexpectedly, they discovered that the fourth ligand is Cys_{69}, the residue to which the methyl group is transferred from phosphotriesters, suggesting that the metal participates directly in the reaction by activating the nucleophilicity of Cys_{69} (Fig. 12) (*58*). Although Ada provided the first example of a protein-(auto)catalyzed process that employs metalloactivation of an amino acid ligand by zinc, evidence has since been presented that a similar mechanism is utilized by protein–cysteine prenyltransferases such as the Ras farnesyltransferase (*59*).

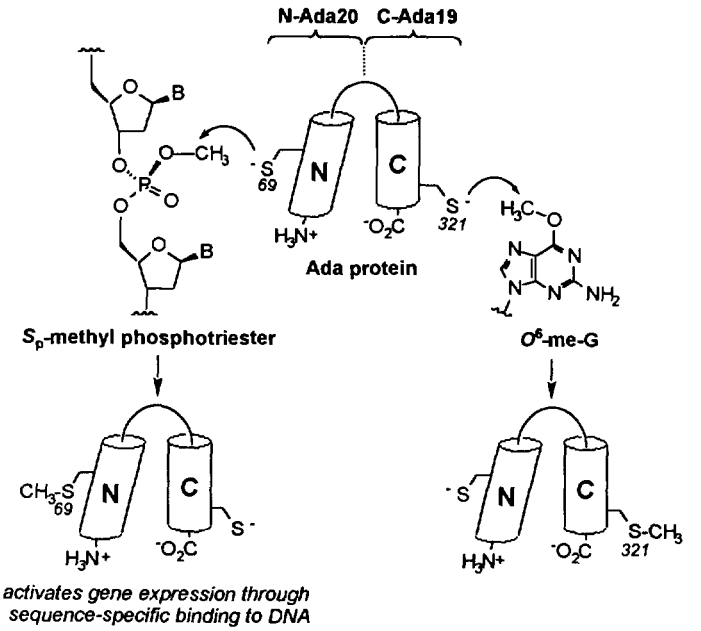

FIG. 11. Physical organization and DNA demethylation reactions autocatalyzed by the *E. coli* Ada protein. Ada contains two domains connected by a protease-sensitive linker. The 20-kDa N-terminal domain repairs the *Sp* diastereomer of methyl phosphotriesters by irreversible transfer to Cys_{69}; the C-terminal domain repairs O^6-methylguanine residues in DNA by direct transfer to Cys_{321}. When produced independently, each domain is fully capable of carrying out its methyl transfer reaction. Methylation of Cys_{69} converts Ada into a strong sequence-specific DNA binding protein; the binding affinity is virtually unaffected by the presence of the C-terminal domain (*55*).

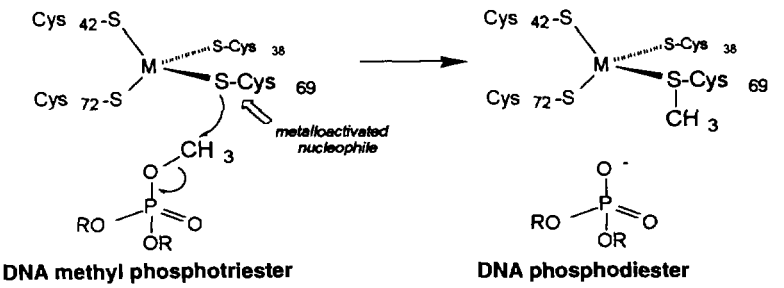

FIG. 12. Autocatalytic activation of nucleophilic attack by Cys_{69} on methyl phosphotriesters by the metal ion in Ada ($M = Zn^{2+}$ or Cd^{2+}).

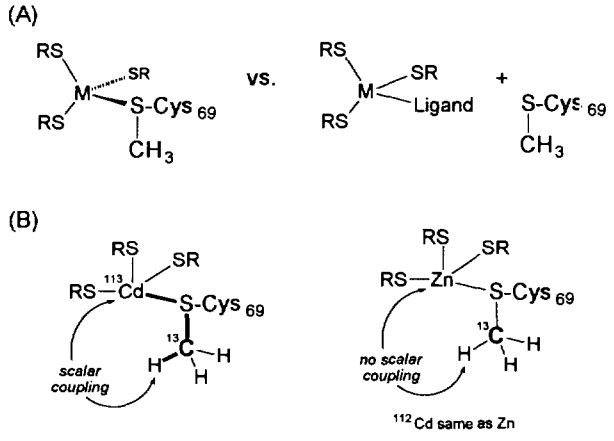

FIG. 13. (A) The two most likely coordination schemes for *S*-me-Cys_{69} in the transcriptionally active form of Ada: the *S*-me-Cys residue remains bound to the metal (left), or it is replaced by a more stable ligand (right). (B) The presence of three-bond coupling between ^{113}Cd and protons of the *S*-methyl group provide a definitive test of the ligation status of *S*-me-Cys_{69}.

Insights into the unusual chemistry of Ada have been gained through elucidation of the solution structure of N-Ada10, a fragment that comprises the entire zinc-binding domain of Ada and repairs methylphosphotriesters as efficiently as the full-length protein, but lacks residues that are necessary for sequence-specific binding to DNA (*60*). These studies reveal that Cys_{69} lies in a shallow depression on the surface of the protein, which accounts in part for the stereochemical preference of the protein for the more accessible S_p methyl phosphotriester. Unlike all other known proteins that possess Cys_4-coordinated zinc, the thiolate sulfur atoms of Ada appear to lack hydrogen bond donors. Dr. Verdine and his co-workers have hypothesized that this allows Ada to maintain the intrinsic reactivity of the zinc-coordinated thiolate at Cys_{69}. On the other hand, proteins that possess structural Cys_4-coordinated zinc clusters must suppress the intrinsic reactivity of their zinc-bound thiolates and do so through hydrogen bonding.

The methyl transfer reaction results in the conversion of a strong zinc ligand, a thiolate anion, to the substantially weaker thioether ligand. An attractive model for the structural switch that converts Ada from a DNA repair protein to a transcriptional activator might thus invoke methylation-promoted exchange of ligands about the metal center (Fig. 13A). In principle, one way to probe the ligand environment about the metal might be simply to compare the ^{113}Cd chemical shift of the methylated protein with that of protein standards having a known ligand constellation. However, reaching an unambiguous answer by this approach is precluded by: (i) the lack of available chemical shift standards for ^{113}Cd coordinated to three thiolates and one thioether, and (ii) the failure to observe an NMR signal for the bound ^{113}Cd in the transcriptionally active form of the protein—the form in which Cys_{69} is S-methylated and the protein is bound to a cognate duplex oligonucleotide. As

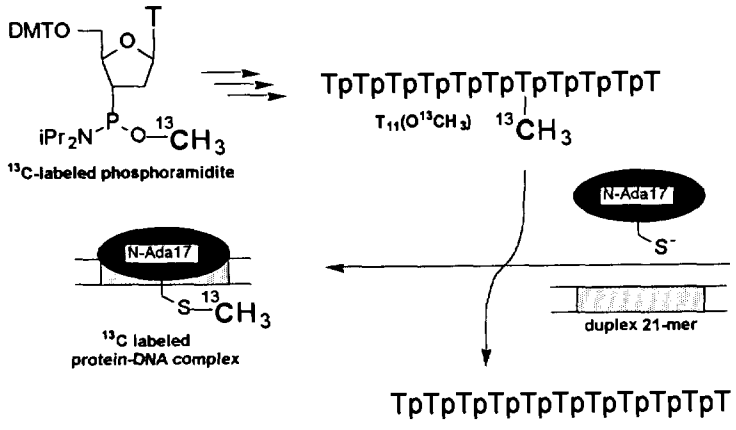

FIG. 14. Synthesis of a single-stranded 11-mer [$T_{11}(O^{13}CH_3)$] containing a single methyl phosphotriester unit, and its use in generation of a specific N-Ada17–DNA complex bearing a ^{13}C-labeled methyl group on Cys_{69}.

an alternative approach, Dr. Verdine's group took advantage of the fact that the *S*-methyl protons on Cys_{69} should be scalar-coupled to the ^{113}Cd only when the *S*–me–Cys_{69} residue is coordinated to the metal; no such coupling should be observed upon ligand exchange of *S*–me–Cys_{69} or when the protein bears the NMR-inactive nuclei ^{65}Zn (predominant form at natural abundance) or ^{112}Cd (Fig. 13B).

In order to permit observation of only the methyl protons of *S*–me–Cys_{69} amidst the vast background of ^1H nuclei in the protein, Dr. Verdine employed isotope-editing techniques, which necessitated the development of a method for labeling only the *S*-methyl group with ^{13}C. Toward this end, they carried out the synthesis of a $^{13}CH_3$-bearing thymine methyl phosphoramidite, which was then incorporated using solid-phase synthesis methods into a single position of a single-stranded T_{11} homopolymer. This phosphotriester-containing oligonucleotide, which is referred to as $T_{11}(O^{13}CH_3)$, was found to be an efficient substrate for the N-terminal domain of Ada (*61*). A 17-kDa N-terminal fragment of Ada (N-Ada17), which abstracts methyl groups and binds DNA as well as the full-length protein, was prepared to contain either ^{113}Cd, ^{112}Cd, or ^{65}Zn. A ^{13}C-methyl group was transferred to Cys_{69} of these three forms of N-Ada17 by treatment with $T_{11}(O^{13}CH_3)$ in the presence of a specific oligonucleotide (Fig. 14). (All Cys_{69}-methylated forms of Ada are highly prone to denaturation, but are significantly stabilized by being bound to a specific oligonucleotide.)

Because of the large size of the complex formed between methylated N-Ada17 and DNA, and the generally small magnitude of the three-bond ^{113}Cd–^1H coupling constant, it was necessary to carry out line-shape analysis of the NMR spectra in order to look for evidence of coupling. Displayed in Fig. 15 are one-dimensional proton cross sections of the ^{13}C-edited proton spectrum of the various ^{13}C-methylated protein–DNA complexes. When the methylated N-Ada17 protein in the complex is charged with the NMR-inactive metal ions ^{65}Zn and ^{112}Cd, the proton signal